Geotech Geol Eng (2023) 41:3403–3425
https://doi.org/10.1007/s10706-023-02465-x

ORIGINAL PAPER

Implementation of an Advanced Constitutive Models for Fine-Grained Soils

Djamel Eddine Bouri · Abdelkader Brahimi · Fatima Zohra Belhassena · Abdallah Krim · Ahmed Arab · Jan Najser · David Mašín

Received: 22 October 2021 / Accepted: 24 April 2023 / Published online: 6 May 2023

Abstract This article presents the effect of silt proportion on the hypoplastic parameters (exponent n, granular hardness hs, exponent α, and exponent β) used for numerical simulation, calculation of emax, and transitional fines content (Fct). Fifteen oedometer tests were carried out at various relative densities (RD = 30, 65, and 80%) to evaluate their effect on the compressibility parameters such as compression index Cc, secant oedometer modulus E_{secant}, and pre-consolidation pressure σ′p. Additionally, ten monotonic undrained triaxial tests were conducted at RD = 65% and RD = 80% to determine the value of the α parameter used in numerical simulation. The results obtained indicate that that the void ratio decreases with the increasing proportion of fine fraction up to 30% and further decreases with an additional increase of fines up to 40% for the three cases of relative densities (RD = 30, 65 and 80%). Additionally, it is shown from our results that the hypoplastic model is able to simulate soil behavior under undrained and oeodometer conditions. It was found that an increase in the α parameter leads to an increase in the dilatancy of the curves observed in the triaxial test. On the other hand, the parameters α and β seem to have no effect on the compressibility curves, and it was necessary to rely on their physical parameters. The transitional fines content (F_{ct})FC_t FC_t depends on the stress level and maximum void ratio, which are calculated from the parameters of the hypoplastic model (e_{io}, hs, ps, n).

D. E. Bouri (✉)
Ecole Nationale Supérieure d'Hydraulique de Blida, GEE, Soumaâ, Algeria
e-mail: d.bouri@ensh.dz

D. E. Bouri
Smart Structures Laboratory, University Center of Ain Témouchent, Ain Témouchent, Algeria

A. Brahimi · A. Krim · A. Arab
Laboratory of Materials Sciences and Environment, Hassiba Ben Bouali University of Chlef, 02000 Ouled Fares, Algeria

A. Brahimi
Institute of Science and Technology, Department of Science and Technology Mila, University Center Abdelhafid Boussouf Mila, Mila, Algeria

F. Z. Belhassena
School of Civil Engineering, Harbin Institute of Technology, Harbin 150090, China

A. Krim
Ibn Khaldoun University of Tiaret, 14000 Tiaret, Algeria

J. Najser · D. Mašín
Faculty of Science, Charles University, Prague, Czech Republic

Keywords Fine content · Hypoplastic · Model · Sand · Void ratio

Abbreviations

G_s	Specific gravity of sand
G_f	Specific gravity of fines
G	Specific gravity of sand-silt mixture
D_{10}	Effective diameter
D_{50}	Average diameter
C_c	Compressibility coefficient
$C_{c\text{-}s}$	Intergranular compressibility coefficient
F_c	Fines content
φ	Internal friction angle
c	Cohesion
e_{max}, Ei	Maximum void ratio
e_{min}	Minimum void ratio
e	Initial void ratio
e_s	Intergranular void ratio
RD	Relative density
R^2	Coefficient of determination
σ’	ŒDometer pressure
e_{i0}	Maximum void ratios
e_{c0}	Critical void ratios
e_{d0}	Minimum void ratios
hs	Granular hardness
α	Exponent
n	Exponent
β	Exponent
φc	Internal friction angle
Esecant	Secant oedometer modulus
σ'_p	Preconsolidation pressure
P'_c	Confining pressure
B	Skempton coefficient
q_{max}	Maximum deviator stress
V_t	Total volume of the mixture
M	Total mass of the mixture
M_{silt}	Mass of the silt
ρ_w	Density of the water
b	Portion of the fine grains that contributes to the active intergrain contacts
hs	Granular hardness
Ps	Mean pressure
H_a	Height of sample at the end of the consolidation under oedometer stress σ'_a
H_b	Height of sample at the end of the consolidation under oedometer stress σ'_b
H_i	Initial height of sample

1 Introduction

Liquefaction of granular soil or loss of soil resistance is considered the most destructive geotechnical phenomenon caused by earthquakes. This phenomenon has received significant attention By engineers in geology and geotechnics such as, Chen et al. (2016), Mase (2020), Belhassena et al. (2021), Ghani and Kumari (2021), Mase et al. (2023). Several researchers have indicated that the liquefaction of granular soils causes settlement of these soils (Belkhatir et al. 2011; Madabhushi and Haigh 2010). The chlef earthquake on october 10, 1980 caused major damage to civil construction, these damage are due to the liquefaction phenomenon and resulting settlement. Several studies have been conducted to estimate the liquefaction strength of Chlef sand, e.g. (Della et al. 2015; Arab 2009; Djafar Henni et al. 2013; Belkhatir et al. 2010; Brahim et al. 2016). All of these studies have evaluated the liquefaction strength of chlef’s granular soil. However, it is also important to study settlement on Chlef sand-silt mixtures because the variation in the amount of fines on a site can cause differential settlement problems. Sand, in nature, is generally found with varying amounts of fines such as clay and silt. The majority of research in the literature has evaluated the impact of the fines fraction (clay, silt) on the mechanical behavior of sand including shear strength, liquefaction resistance, pore water pressure, volumetric strain, mechanical parameters c and φ. Chang et al. (1982) showed that the liquefaction resistance of clean sand was influenced by the average diameter (D_{50}) and the uniformity coefficient (Cu). (Ishihara et al. 1990; Ishihara 1993; Zlatovic and Ishihara 1995) studied the deviator-strain behaviour of loose Toyoura sand-silt mixture using three sample preparation methods, dry deposition (DD), moist placement (MP) and by water sedimentation (WS). Their results indicated that fines content and sample preparation method have an effect on peak resistance and residual strength.

Lade and Yamamuro (1997) and Covert and Yamamuro (1997) found that increasing the fines content of clean sand can increase the potential for liquefaction up to a certain maximum level, beyond which the behavior of the fines dominate the undrained soil behavior. Amini (2000) showed that increasing the fines content increases the liquefaction resistance of the sand–silt mixture. Arab et al. (2011), Arab et al.

(2014) indicated that increasing the fines content decreases the liquefaction resistance and the friction angle of Chlef sand–silt mixtures. Huang et al. (2004) and Rahman and Lo (2014) reported that the liquefaction potential of clean sands increases with increasing fines content for FC ≤ 25%. Najjar et al. (2015) found that the cohesion increases with increasing clay content from 0 to 40%, while the angle of friction decreases.

Monkul et al. (2017) reported that the grading characteristics of sand have a significant influence on the static liquefaction potential of clean and silty sands. Akhila et al. (2019) conducted a series of undrained cyclic triaxial tests on sand–silt mixtures. Their results showed that at constant void ratio, the liquefaction resistance of sand-fine mixtures decreases with the addition of non-plastic fines up to 40%.

Porcino et al. (2019) showed that an increase in fines significantly influences the undrained monotonic response of sand when tested at a constant relative density. Up to a transition fines content, the undrained behavior of the sand–silt mixture becomes more contractive and gets more pronounced with increasing fines content, resulting in a reduction in peak and steadystate strengths. (Enomoto 2019) fount that the undrained strength of sand-silt mixtures decreases with increasing fines content from 0 to 50%. Mahmoudi et al. (2022) carried out undrained tests on sand-silt samples and their results indicated that the resistance to liquefaction decreases with an increase in fines content from 0 to 50%, while the pore pressure increases. Goudazy et al. (2022) demonstrate that for both types of plastic fines, an increase in the fines fraction leads to a more contractive response of undrained behavior and lower values of mobilized deviatoric stress.

However, few studies in the literature have focused on the impact of fines proportion on the compressibility behavior of liquefied soils. Bouri et al. (2021) conducted oedometric tests on sand-silt samples and concluded that the initial conditions (relative density and preparation method) have an influence on the compressibility parameters (Cc and Cc-s),particle size (D_{10}, D_{50} and C_u) and the transitional fines content F_{ct}. Monkul and Ozden (2007) demonstrated that the initial conditions, percentage of kaolinite and applied oedometric pressure have an impact on the compressibility index and granular compressibility index (Cc and Cc-s). Their tests showed that until a certain quantity of fines (transitional fines content), the intergranular void ratios (e_s) are completely filled by fine fraction, the compressibility behavior of the sand-fine mixtures is largely dominated by the granular matrix (sand). When the percentage of fines exceeds (F_{ct} FC_tFC_t), the compressibility behavior is dominated by the fine matrix. (Yin 1999; Cabalar and Hasan 2013; Cfa et al. 2013) demonstrated that the fine fraction has a strong on the compressibility parameters. Their tests showed that the compressibility of the soil increases with an increase in fines content. (Lupogo 2012) conducted oedometer tests on sand-silt mixtures with various types of clay. The results indicated that the compressibilty behavior is not influenced by the nature of fine up to F_{ct} and its plasticity. However, above Fct, the fine fraction controls the compressibility of the mixture and varies according to the chemical formulation of the fines. Thevanayagam and Mohan (2000) studied the consolidation behavior of granular soil mixed with plastic fines. Their results indicate that the transitional fine content is between 20 and 30% of plastic fines. They showed that for a fine content ≤ 10% the granular matrix (sand) dominates the compressibility of the mixture whereas for a fraction of fines ≥ 40% the fine matrix controls the compressibility of the mixture. Based on the results of (Monkul and Ozden 2007; Cabalar and Hasan 2013) we conclude that the intergranular void ratio is the ideal parameter to estimate the mechanical behavior of sand-silt or sand-clay mixtures. The calculation of the interganular void index was proposed by Kuerbis et al. (1988)as follows:

$$e_s = \frac{V_T \cdot G_s \cdot \rho_w - (M - M_{silt})}{(M - M_{silt})} \tag{1}$$

While Thevanayagam (1998), Thevanayagam and Martin (2002) used Eq. (2) and (3) for estimation the intergranular void ratio:

$$e_s = \frac{e + F_c/100}{1 - F_c/100} \tag{2}$$

$$e_s = \frac{e + (1-b)F_c/100}{1 - (1-b)F_c/100} \tag{3}$$

where (es) is the intergranular voids ratio, (Fc) the fines content, (e) the ratio of voids and (b) is the portion of the fine grains that contributes to the active intergrain contacts.

The hypoplastic model proposed by (Wolffersdorff 1996) is the best known model for simulating the behavior of granular soils, the model requires 8 material parameters (φ_c, n, hs, e_{i0}, e_{d0}, e_{c0}, α and β). Several researchers have used the hypoplastic model as a constitutive model for granular soil including (Gudehus 1996; Herle and Gudehus 1999; Mašín 2012a; Masin 2019, Najser et al. 2012; Mohammadi and Ardakani 2020). In this study, several hypoplastic model parameters (hs, n, α, β, e_{i0}, e_{co}, e_{d0} and φ_c) were used. First we estimated the influence of the fines proportion on the hypoplastic parameters (hs, n and α). Secondly we calculated the maximum void ratio e_{max} using (Gudehus 1996) equation:

$$e_i = e_{i0}\exp\left[-\left(\frac{3ps}{hs}\right)\right]^n \tag{4}$$

Monkul and Ozden (2007) used a constant maximum void ratio e_{max} (e_{max} at 0 kPa oedometer pressure) to determinate the transitional fine content. However, in reality, according to (Gudehus 1996) the maximum void ratio e_{max} is not fixed and depends on the applied oedometer pressure. e_{max} changes with the variation of the oedometer pressure from 25 to 800 kPa. Therefore, the value of transitional fine content changes and the compressibility behavior of sand-silt mixtures also changes.

This study aims to investigate the impact of the silt fraction (F_c) and relative density (RD) on the hypoplastic parameters model. Then, the transition fine content (F_{ct})FC_t FC_t for the three cases of relative density (RD = 30%, RD = 65% and RD = 80%) was compared based on the concept of the intergranular void ratio (when $e_s = e_{max-c}$) corresponding to Monkul and Ozden (2007). Finally, the influence of the fine content on the compressibility parameters Cc, E_{secant} and σ'_p has been evaluated.

2 Materials and Experimental Procedure

The tests were performed on a rounded Chlef sand mixed with Chlef silt. Chlef sand and silt have been used in several research studies (Belkhatir et al. 2012; Bouri et al. 2019; Brahim et al. 2016; Brahim et al. 2018; Krim et al. 2021; Nougar et al. 2021, Brahimi et al. 2022, Nougar et al. 2022).

Minimum and maximum dry unit weight were determined based on (ASTM D 4254-00 2002) and (ASTM D 4253-00 2002), Specific gravity for clean Chlef sand is G_s = 2.65 and 2.68 for Chlef silt,. The effective diameter (D_{10}), the average diameter (D_{50})

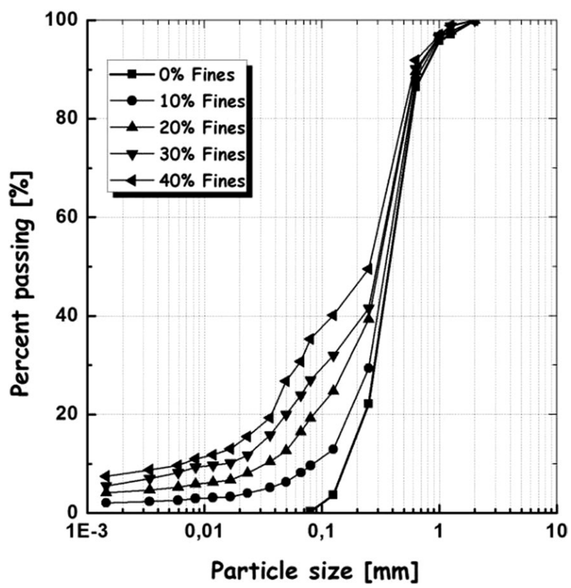

Fig. 1 Particle size distribution curves for the different sand-silt mixtures

Table 1 Physical parameters of sand-silt mixtures

Materials	F_c (%)	G_s	D10 (mm)	D50 (mm)	C_u	e_{min}	e_{max}
Clean sand	0	2.650	0.17	0.41	2.82	0.623	0.848
	10	2.653	0.08	0.38	5.28	0.487	0.811
Sand-silt mixtures	20	2.656	0.04	0.33	9.80	0.455	0.776
	30	2.659	0.03	0.32	13.31	0.421	0.749
	40	2.662	0.02	0.25	15.17	0.489	0.803
Silt	100	2.68	–	0.03	–	0.852	1.345

and the uniformity coefficient (C_u)C_U C_U C_U are given in Table 1, and the particle size distribution curve for the different mixtures used in this study is shown in Fig. 1.

2.1 Oedometer Test Procedure

These tests were carried out by Bouri et al. (2021) using an odometer device of 70 mm with a diameter and a height of 20 mm to investigate the compressibility behavior. The tests were conducted according to the standard (ASTM D 2435/ D 2435 M 1997). The sand-silt mixture was placed in the œdometer ring and densified by dynamic blows until the desired void ratio was reached (RD = 30%, RD = 65% and RD = 80%). Then, the top cap was installed and the sample was flooded to saturate it. The loading stage started after 24 h of saturation. The applied oedometer pressure was doubled every 24 h (for example from 25 to 50 kPa and from 50 to 100 kPa up to 800 kPa).The sample preparation method was the same for all samples.

Fig. 2 Triaxial apparatus used in this study

2.2 Triaxial Test Procedure

Figure 2 shows the triaxial apparatus used in this study. Cylindrical specimens with a diameter of 30 mm and a height of 70 mm were formed using the moist tamping technique Benahmed et al. (1999). The sand was first mixed with the silt, and then 3% de-aired water was added using the moist tamping method as described by (Castro 1969). The wet sand-silt mixture was divided into several layers to ensure a good grain distribution, and each layer was compacted to reach the target void ratio or relative density which were RD = 65% and RD = 80%.

Saturation of the samples was achieved using carbon dioxide CO_2 technique. The skempton coefficient B value obtained in our test was 0.95. The confining pressure used for our tests was 200 kPa.

3 Numerical Simulation of the Oedometer Test and Triaxial Test:

The numerical simulation using the hypoplastic model for granular materials was performed in the Plaxis finite element software. The model is based on eight parameters α, β, hs, ps, n, e_{i0}, e_{d0} and e_{c0}. The vertical deformation versus time curve for the oedomter test (Fig. 3), and deviator stress versus deformation for triaxial test (Fig. 4) were selected. The hypoplastic model for granular materials was implemented through the user defined subroutine usermod.

4 Results and Interpretation

4.1 Effect of Fines Proportion on the Compressibility Behavior of Chlef Sand

Variation in void ratio (e) with oedometer pressure (σ') are presented for three cases of relative densities (30%,65% and 80%) and different fine fraction (Fc) in Fig. 5a, b. The samples prepared at relative density of RD = 30% exhibited larger void ratios compared to those prepared at relative density RD = 65% and RD = 80%, this difference is due to the lower compaction and higher void ratio for the samples prepared at RD = 30%. For loose samples (RD = 30%), the difference between the largest and smallest value

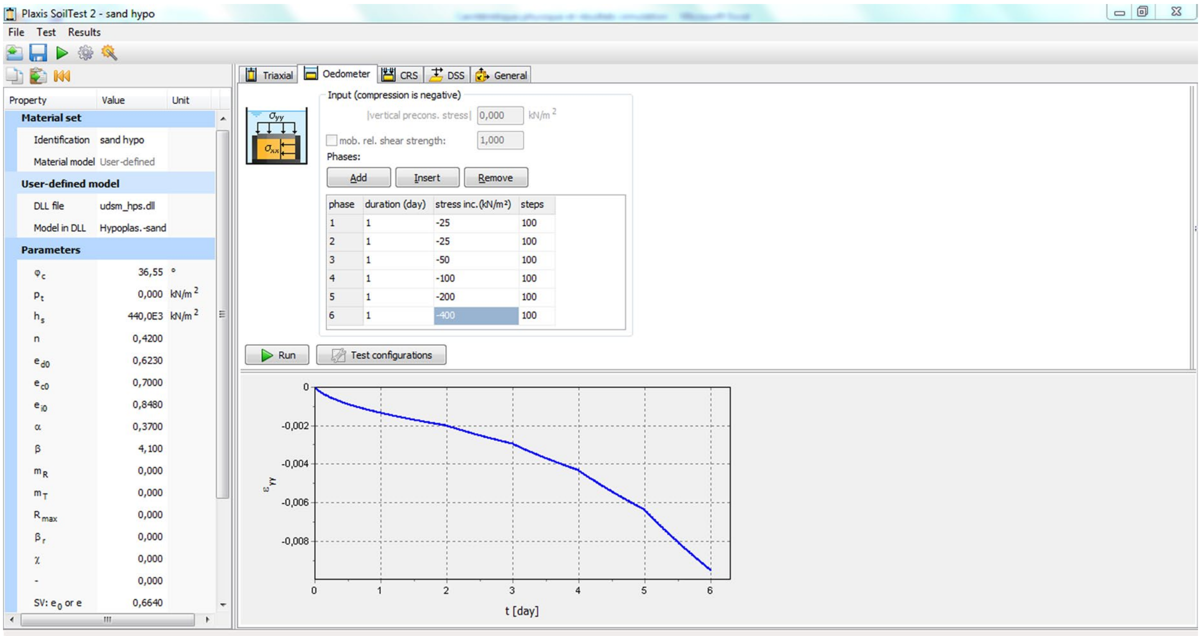

Fig. 3 Example of oedometer test simulation in Plaxis 3D

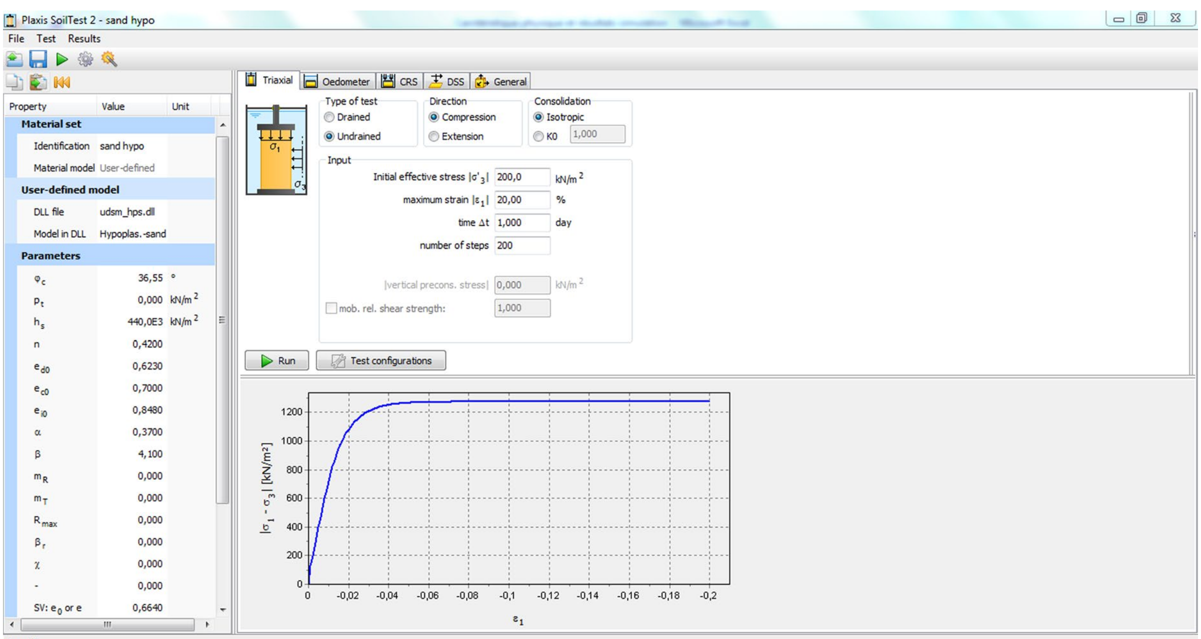

Fig. 4 Example of triaxial test simulation in Plaxis 3D

of the void ratio is equal to Δe = 0.14 for an applied oedometer pressure of 25 kPa, whereas for an applied oedometer pressure of 800 kPa the value of Δe was equal to 0.24.

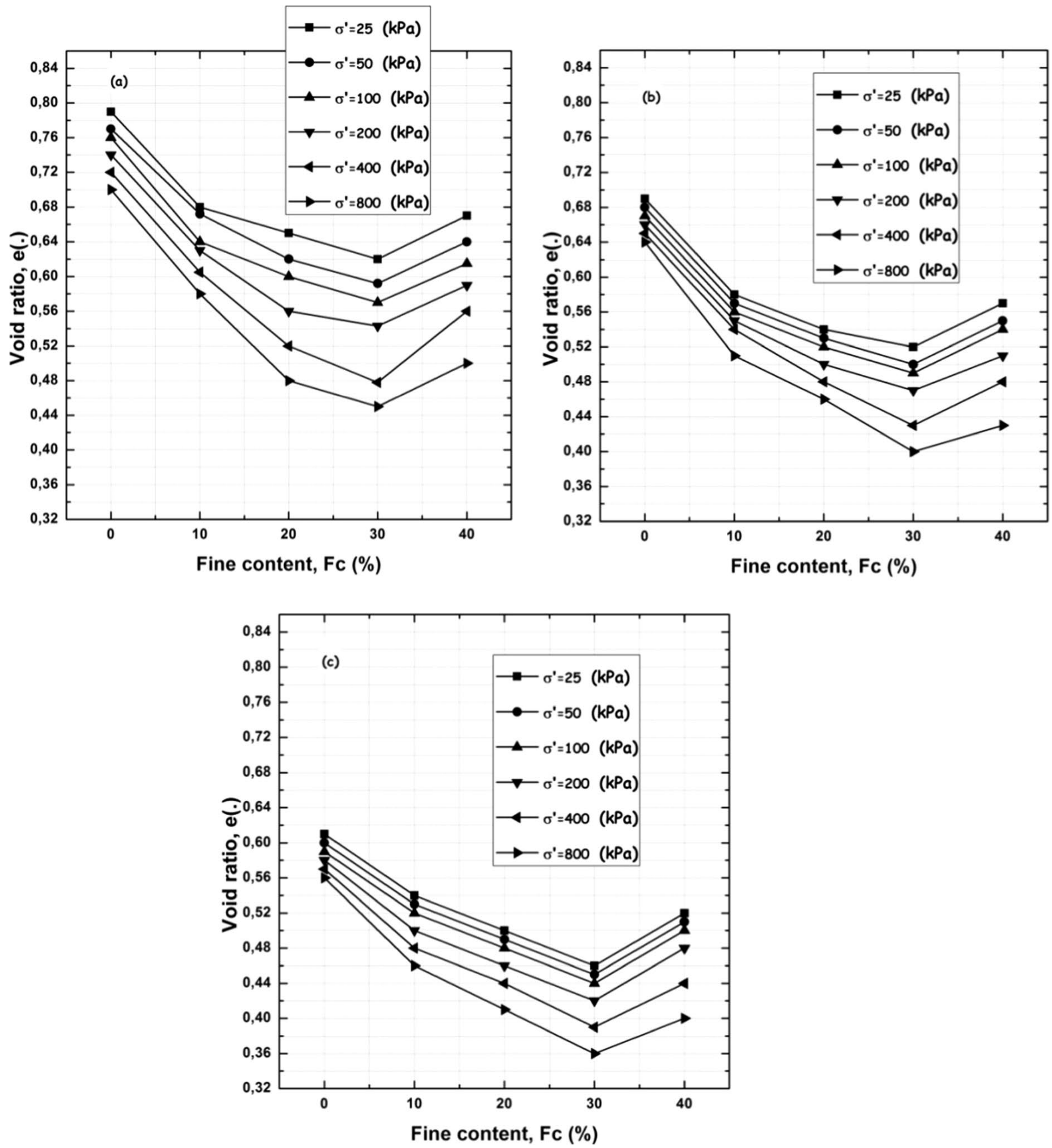

Fig. 5 The change in the global void index (e) as a function of the fine content (Fc). **a** Loose state (RD = 30%), **b** Medium dense state (RD = 65%), **c** Dense state (RD = 80%)

For medium dense samples (RD = 65%), the difference between the largest and smallest values of the void ratio is equal to Δe = 0.12 for an applied oedometric pressure of 25 kPa, whereas for an applied oedometer pressure of 800 kPa the value of Δe was equal to 0.21, this difference is due to the difference in the applied oedometer pressure. However, for the dense samples (RD = 80%) the difference between the largest and smallest value of the void ratio is equal to Δe = 0.09 for an applied oedometer pressure of 25 kPa, whereas for an applied oedometer pressure of 800 kPa the value of Δe was equal to 0.16. The differences in the Δe values between the samples prepared at loose state (RD = 30%), medium dense state (RD = 65%) and dense state (RD = 80%) is due to the difference in compaction and consequently a difference between the Δe values. The results indicate that the void ratios decrease with an increase in fines content up to Fc = 30% for all three relative densities (RD = 30%, RD = 65%, and RD = 80%). However, beyond this point, the void ratios increase with a further increase in fines content. The results indicate that the representation of compressibility behavior by the global void ratio is not satisfactory.

(Monkul and Ozden 2007; Belkhatir et al. 2010) have shown that the behavior of sand-fine mixtures cannot be represented by the global void index. When sand contains fines, the global void index (e) is not able to characterize soil behavior. Indeed, until a certain fines proportion, F_c, fines fill the void spaces between the sand grains and do not influence the mechanical behavior of the sand-fine mixture. According to the insufficient results found of the global void index, the use of the intergranular void index seems to be essential.

Monkul and Onal (2006) suggested the Eq. (5) for calculation of the intergraular void index:

$$e_s = \frac{e + G \cdot Fc/Gf \cdot 100}{G/Gs \ \cdot (1 - Fc/100)} \tag{5}$$

G_s and G_f are the specific gravity of sand and the fines, respectively. G is the specific gravity of sand-silt mixture.

Figures 6a, b and c illustrate the change in the intergranular void index (e_s) versus fine content (Fc) for different œdometer pressure (σ′). The intergranular void index (e_s) was calculated using Eq. 5. The results illustrate that an increase in compaction and applied œdometer pressure (σ′) decreases the void ratio between sand grains (intergranular void index e_s). Furthermore, the results show that an increase in silts content from 0 to 40% increases the intergranular void index (e_s).

4.2 Influnece of Fine Proportion on the Hypoplastic Parameters

Grading characteristics and angularity of sand are known to influence hypoplastic parameters of granular soils, such as exponent n, granular hardness hs, exponent α and exponent β. Herle and Gudehus (1999) found that the hypoplastic parameters (exponent n, granular hardness hs, exponent α) are influenced by the angularity of the sand and by its grading characteristics (Cu and D_{50}). In this part the effect of silt on the hypoplastic parameters (exponent n, granular hardness hs, exponent α and exponent β) of granular soils will be evaluated (Tables 2, 3).

The α parameter controls the critical angle φ_c and the peak friction angle φ_p. For this reason, ten triaxial tests were performed on medium dense and dense samples to determine the critical angle of friction (φ_c) and the peak angle of friction (φ_p) (Figs. 7 and 8, Table 4) for the calculation of the α parameter. The results from the undrained triaxial tests show that the peak friction angle and the critical friction angle decrease with increasing silt proportion in sand. The exponent α can be calculated from Eq. (6) suggested by Herle and Gudehus (1999):

$$\alpha = \frac{ln\left[6\frac{(2+K_p)^2+a^2K_p(K_p-1-\tan\nu_p)}{a(2+K_p)(5K_p-2)\sqrt{4+2(1+\tan\nu_p)2}}\right]}{ln\left((e-e_d)/(e_c-e_d)\right)} \tag{6}$$

The parameter Kp is calculated as a function of the peak friction angle φ_p using Eq. (7):

$$K_p = \frac{T_1}{T_2} = \frac{1+\sin\varphi_p}{1-\sin\varphi_p} \tag{7}$$

The parameter a is calculated as a function of the critical friction angle φ_c using Eq. (8):

$$a = \frac{\sqrt{3}(3 - sin\varphi_c)}{2\sqrt{2}sin\varphi_c)} \tag{8}$$

The peak dilatancy angle is calculated using Eq. (9):

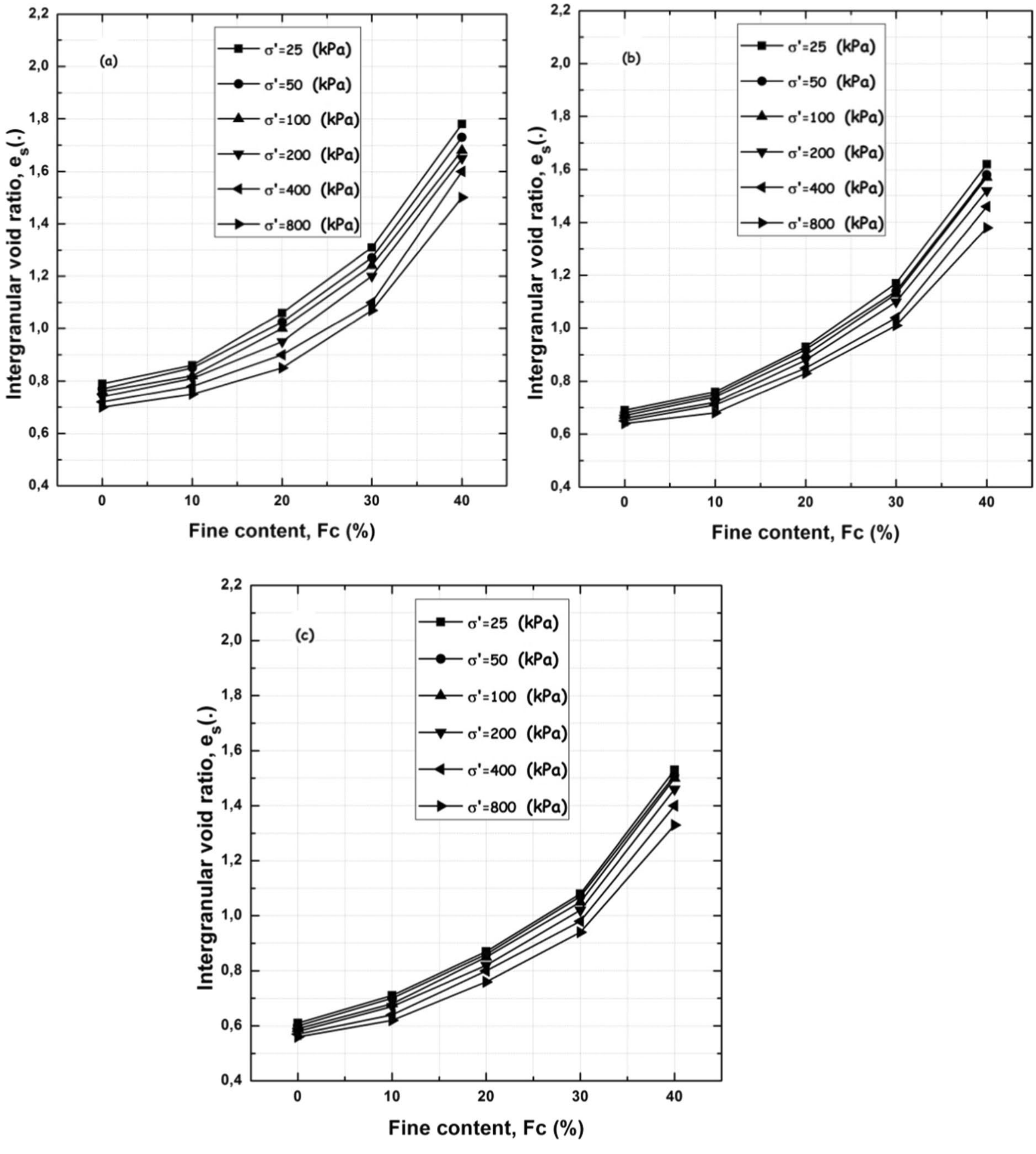

Fig. 6 The change in the intergranular void index as a function of the fine content (Fc). **a** Loose state (RD = 30%), **b** Medium dense state (RD = 65%), **c** Dense state (RD = 80%)

Table 2 Summary of oedometer tests

Materials	Fc (%)	σ′ (kPa)	e for RD = 30%	e for RD = 65%	e for RD = 80%
Clean sand	0	25	0.79	0.69	0.61
		50	0.77	0.68	0.60
		100	0.76	0.67	0.59
		200	0.74	0.66	0.58
		400	0.72	0.65	0.57
		800	0.70	0.64	0.56
Silty sand	10	25	0.680	0.58	0.54
		50	0.720	0.57	0.53
		100	0.64	0.56	0.52
		200	0.60	0.55	0.50
		400	0.59	0.54	0.48
		800	0.58	0.51	
Silty sand	20	25	0.63	0.54	0.50
		50	0.62	0.53	0.49
		100	0.60	0.52	0.48
		200	0.56	0.50	0.46
		400	0.52	0.48	0.44
		800	0.48	0.46	0.41
Silty sand	30	25	0.62	0.52	0.46
		50	0.59	0.50	0.45
		100	0.57	0.49	0.44
		200	0.54	0.47	0.42
		400	0.47	0.43	0.39
		800	0.41	0.40	0.36
Silty sand	40	25	0.67	0.57	0.52
		50	0.64	0.55	0.51
		100	0.61	0.54	0.50
		200	0.59	0.51	0.48
		400	0.56	0.48	0.44
		800	0.47	0.43	0.40

Table 3 Summary of undrained triaxial tests

Test No	Materials	Fc (%)	RD (%)	P’c (kPa)	B (%)	q_{max} (kPa)
1	Clean sand	0	65	200	95	878.360
2	Clean sand	0	80	200	95	1260.56
1	Silty sand	10	65	200	95	786.51
2	Silty sand	10	80	200	95	1106.87
1	Silty sand	20	65	200	95	670.14
2	Silty sand	20	80	200	95	878.84
1	Silty sand	30	65	200	95	540.98
2	Silty sand	30	80	200	95	775.62
1	Silty sand	40	65	200	95	416.73
2	Silty sand	40	80	200	95	510.63

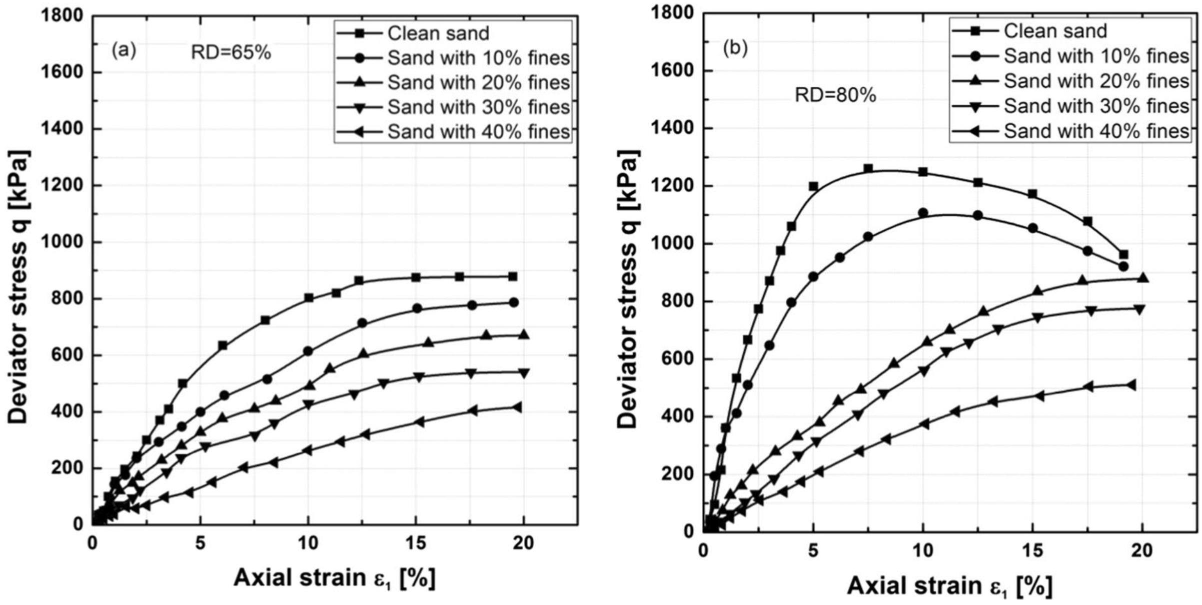

Fig.7 Change in deviator stress as function as axial strain. **a** Medium dense samples (RD = 65%) **b** Dense samples (RD = 80%)

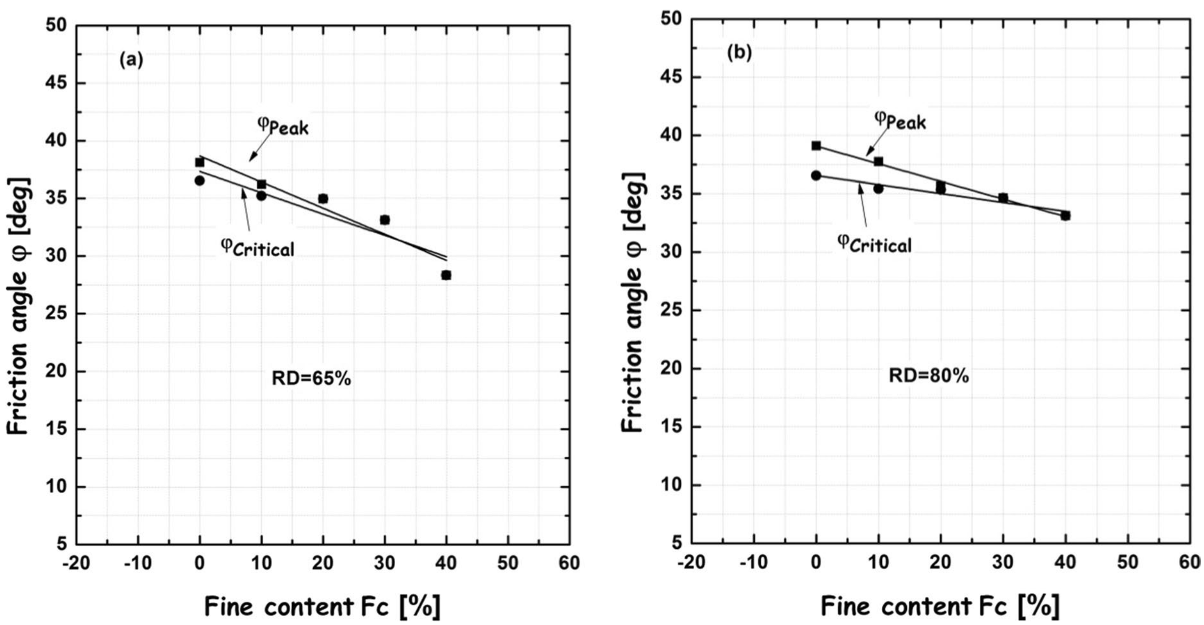

Fig. 8 Variation of peak and critical friction angle versus the fine content. **a** Medium dense samples (RD = 65%) **b** Dense samples (RD = 80%)

Table 4 values of peak and critical friction angle for dense samples (RD = 80%)

Percentage of fine content (%)	Peak friction angle (φ_{peak})	Critical friction angle ($\varphi_{critical}$)
0	39.11°	36.55°
10	37.75°	35.43°
20	35.66°	35.36°
30	34.65°	34.65°
40	33.12°	33.12°

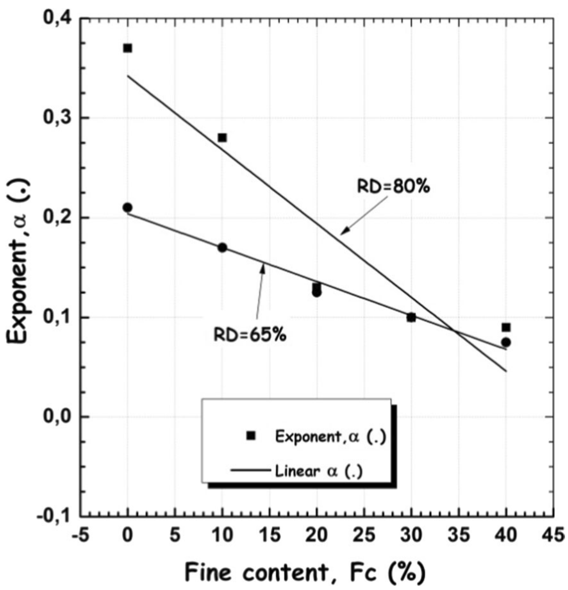

Fig. 9 Variation of exponent (α) versus the fines content (F_c)

$$tanv_p = 2\frac{K_p - 4 + 5AK_p^2 - 2AK_p}{(5K_p - 2)(1 + 2A)} \tag{9}$$

With:

$$A = \frac{a^2}{(2 + K_p)^2}\left[1 - \frac{K_p(4 - K_p)}{(5K_p - 2)}\right] \tag{10}$$

Figure 9 illustrate the change in the exponent (α) with the fines proportion (F_c). It is noted that the exponent (α) increases linearly with the addition of the silts proportion (F_c). These results suggest that the parameter (α) is affected by the amount of silt added to the sand, indicating the necessity of taking into account the quantity of fines present in the sands to have a better numerical simulation quality.

The β parameter influences the dimension of the response envelope (both bulk and shear strength).The

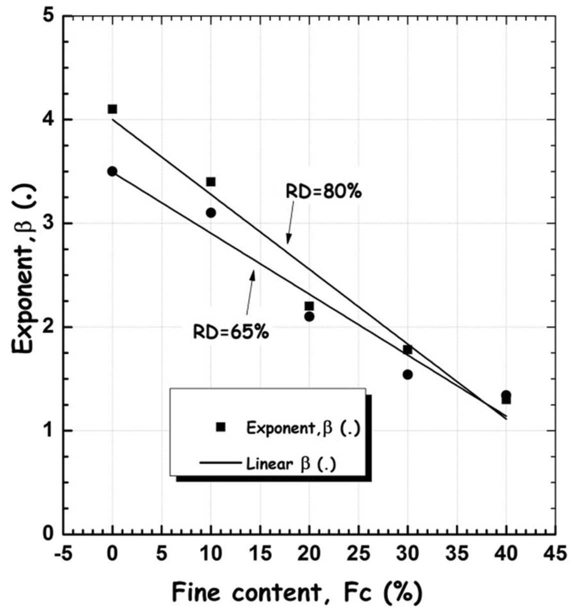

Fig. 10 Variation of exponent (β) versus the fines content (Fc)

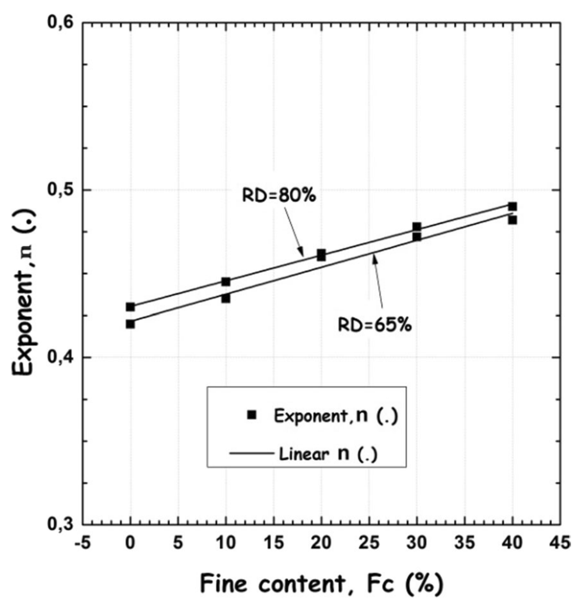

Fig. 11 Variation of exponent (n) versus the fines fraction (Fc)

exponent β can be calculated from Eqs. (11), (12) and (13) according to Herle and Gudehus (1999):

$$\beta = \frac{\ln\left[E\frac{3+a^2-f_{d0}a\sqrt{3}}{3+a^2-f_d a\sqrt{3}}\frac{e_i}{1+e_i}\frac{n}{hs}\left(\frac{3ps}{hs}\right)^{n-1}\right]}{\ln\left(e_i/e\right)} \tag{11}$$

$$f_{d0} = \frac{e_{i0} - e_{d0}}{e_{c0} - e_{d0}} \tag{12}$$

$$f_d = \left(\frac{e - e_d}{e_c - e_d}\right)^{\alpha} \tag{13}$$

Figure 10 shows the variation of the exponent (β) with the silts proportion (F_c), the figure shows that the exponent (β) decreases linearly with the increase of the silts proportion (F_c).hs and n are considered as related parameters for numerical modeling of the compressibility behavior, Hs and n control the shape of limiting void ratio curves (normal compression lines and critical state line) and can be determined from Eq. (14) and (15) according to Herle and Gudehus (1999):

$$n = \ln\left[\frac{\lambda 2 \cdot e1}{\lambda 1 \cdot e2}\right] \ln\left(\frac{ps1}{ps2}\right) \tag{14}$$

$$Hs = 3ps\left(\frac{n * e}{\lambda}\right)^{1/n} \tag{15}$$

Figure 11 shows the variation of the exponent (n) versus the fines proportion (F_c), it is noted that the exponent (n) increases linearly with the increase of the fines proportion (F_c)..

4.3 Validation of the Calculated Hypoplastic Parameters Model

Figure 12a and b show the comparison of the numerical and laboratory results of the oedoemeter test at diferent fine contents. The comparison demonstrates that the hypoplastic model can simulate the compressibility behavior. According to Fig. 12, the results of the numerical simulation are in good agreement with the tests carried out in the laboratory. We note that the hypoplastic model for granular materials predicts well the variation of the void ratio versus oedometer applied pressure found in the laboratory at different densities and showed the precise estimation of the parameter values. Parameters α and β seem to have no effect on the compressibility curves and it is necessary to rely on their physical parametres. A similar observation was found by Masin (2019), Mohammadi-Haaji and Ardakani (2020).

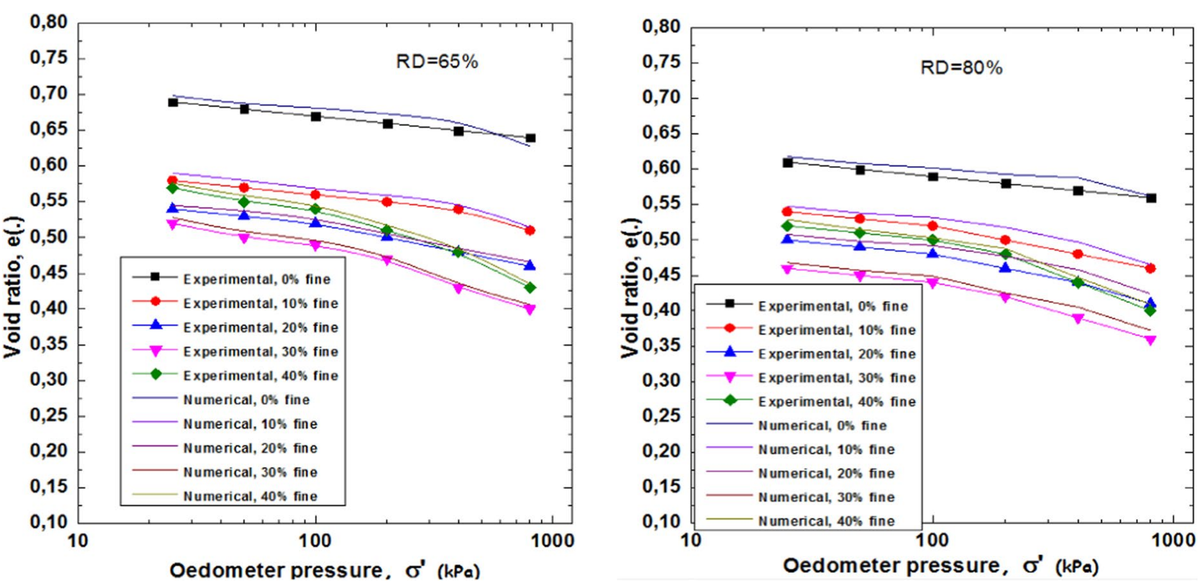

Fig. 12 Comparison of experimental oedometer test with the numerical data

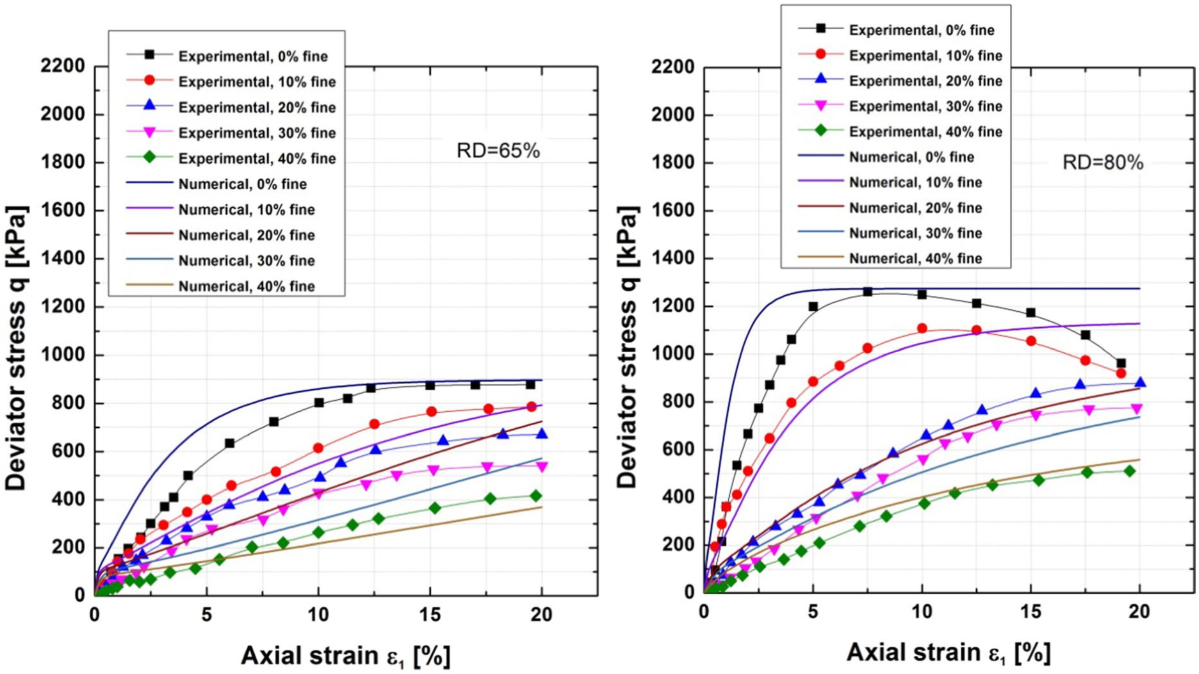

Fig. 13 Comparison of experimental triaxial test with the numerical data

Table 5 Parameters of medium dense sand-silt mixtures used into the model

Materials	φ_c	n	hs (GPa)	e_{c0}	e_{d0}	e_{i0}	α	β	e
Clean sand	36.55	0.420	0.35	0.700	0.623	0.848	0.210	3.50	0.672
	35.23	0.435	0.25	0.670	0.487	0.811	0.170	3.10	0.637
Sand-silt mixtures	34.97	0.460	0.24	0.645	0.455	0.776	0.125	2.15	0.600
	33.13	0.472	0.18	0.630	0.421	0.749	0.100	1.54	0.575
	28.33	0.482	0.20	0.675	0.489	0.803	0.070	1.34	0.620

Table 6 Parameters of dense sand-silt mixtures used into the model

Materials	φ_c	n	hs (GPa)	e_{c0}	e_{d0}	e_{i0}	α	β	e
Clean sand	36.55	0.430	0.440	0.700	0.623	0.848	0.370	4.10	0.664
	35.43	0.445	0.037	0.670	0.487	0.811	0.280	3.40	0.572
Sand-silt mixtures	35.36	0.462	0.011	0.645	0.455	0.776	0.130	2.20	0.515
	34.65	0.478	0.007	0.630	0.421	0.749	0.105	1.78	0.472
	33.12	0.490	0.005	0.675	0.489	0.803	0.090	1.30	0.520

Figure 13a and b show the comparison between the numerical and laboratory triaxial test results. It can be seen that the curve for the proposed α and β value is in good agreement with the experimental curves. A greater α leads to a larger initial deviator stress, and it is very clear that the increase in the α parameter increases the dilatancy of the curves. A similar observation was found by Masin (2019), Mohammadi-Haaji and Ardakani (2020) (Table 5, 6).

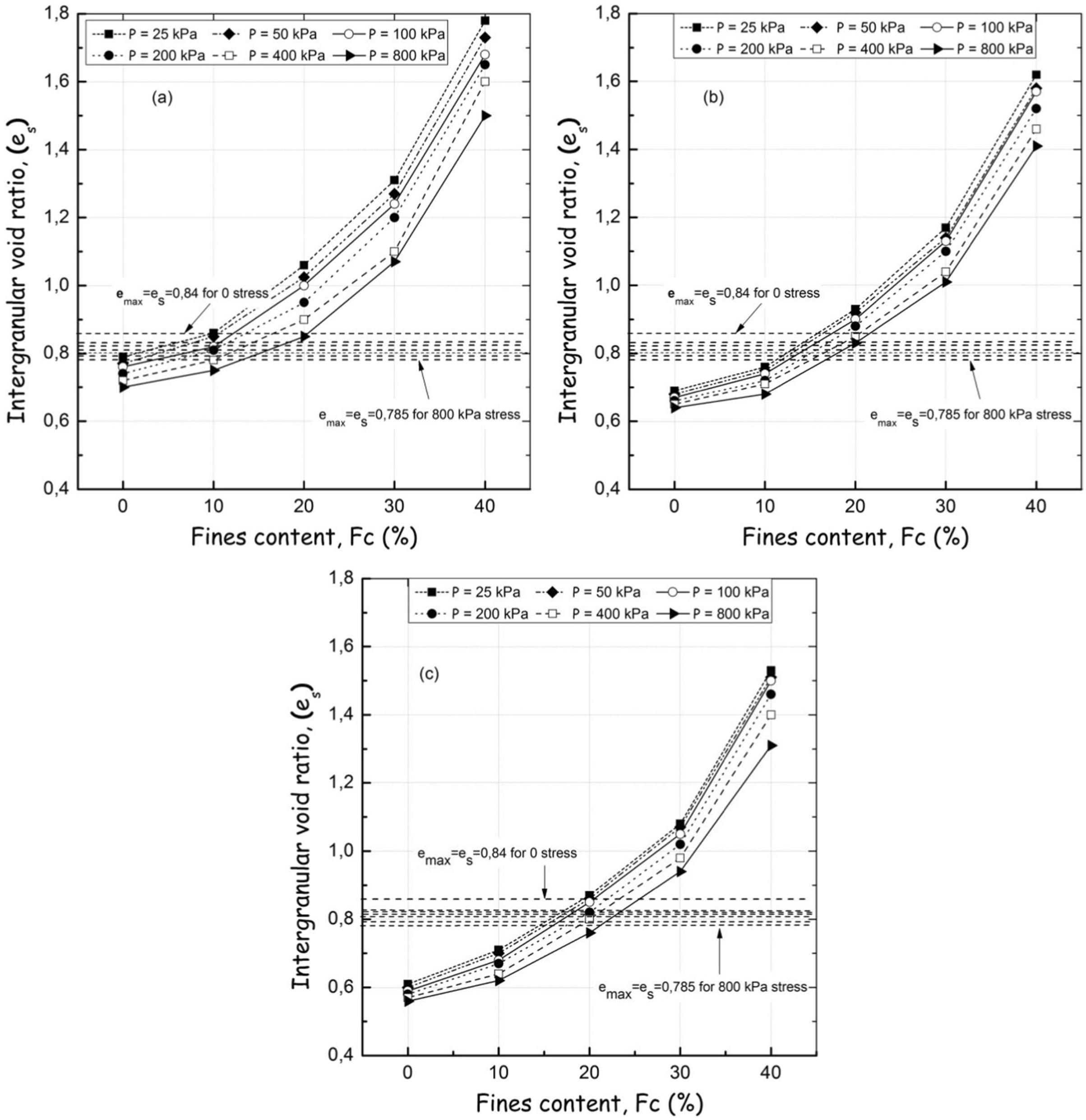

Fig. 14 Variation in the intergranular void ratio versus the fines fraction. **a** RD = 30%, **b** RD = 65%, **c** RD = 80%

4.4 Transitional Fine Content

We know that the loosest state of sand comes at the maximum void ratio. This maximum void index is used in the calculation of Fct. According to (Gudehus 1996) e_{max} is not constant, which actually itself depends on oedometer pressure (σ′). Based on the notion of the intergranular void index (when $e_s = e_{max-c}$), corresponding to the determination of the transition fines content by Monkul and Ozden (2007), Fig. 14a–c, represent the change in the intergranular void index with fine proprotion under

Table 7 Content transition (FC_t) for sample with RD = 30%, under different œdometric pressures for each emax calculate from equation of Gudehus (1996)

Oedometer stress, P (kPa)	Value of FC_t for $e_{max}=0.84$	Value of FC_t for $e_{max}=0.828$	Value of FC_t for $e_{max}=0.823$	Value of FC_t for $e_{max}=0.817$	Value of FC_t for $e_{max}=0.808$	Value of FC_t for $e_{max}=0.797$	Value of FC_t for $e_{max}=0.785$
25 kPa	9.38	6.14	5.03	4.25	2.90	0.88	0.18
50 kPa	10.29	7.46	5.94	4.32	3.51	2.50	1.90
100 kPa	12.41	10.99	10.18	7.27	4.72	4.017	3.72
200 kPa	13.32	11.05	10.29	9.22	8.17	7.25	5.94
400 kPa	16.45	14.94	14.23	13.32	12.21	11.41	9.88
800 kpa	20.50	18.58	8.38	17.77	15.95	14.44	13.12

Table 8 Content transition (FC_t) for sample with RD = 65%, under different œdometric pressures for each e_{max} calculate from equation of Gudehus (1996), (Adapted from Bouri et al. 2021)

Oedometer stress, P (kPa)	Value of FC_t for $e_{max}=0.84$	Value of FC_t for $e_{max}=0.828$	Value of FC_t for $e_{max}=0.823$	Value of FC_t for $e_{max}=0.817$	Value of FC_t for $e_{max}=0.808$	Value of FC_t for $e_{max}=0.797$	Value of FC_t for $e_{max}=0.785$
25	15.69	14.30	13.65	13.13	12.27	11.84	11.20
50	16.55	14.84	14.41	13.87	13.23	12.37	11.73
100	17.51	15.69	15.05	14.41	13.87	13.23	12.48
200	18.69	16.98	16.44	15.69	15.16	14.52	13.76
400	20.51	18.58	18.15	17.09	16.76	15.90	15.05
800	21.68	20.08	19.34	18.91	18.15	17.40	16.66

Table 9 Content transition (FCt) for sample with RD = 80%, under different œdometric pressures for each emax calculate from equation of Gudehus (1996)

Oedometer stress, P (kPa)	Value of FC_t for $e_{max}=0.84$	Value of FC_t for $e_{max}=0.828$	Value of FC_t for $e_{max}=0.823$	Value of FC_t for $e_{max}=0.817$	Value of FC_t for $e_{max}=0.808$	Value of FC_t for $e_{max}=0.797$	Value of FC_t for $e_{max}=0.785$
25 kPa	19.01	16.98	16.76	15.80	15.69	15.05	14.30
50 kPa	19.43	17.94	17.29	16.76	16.33	15.58	14.74
100 kPa	20.19	18.58	18.05	17.09	17.01	16.66	15.69
200 kPa	21.90	20.08	19.86	18.80	18.37	18.15	17.20
400 kPa	23.18	21.36	21.25	20.64	20.08	19.76	18.91
800 kpa	25.43	23.50	23.30	22.60	22.22	22.01	21.47

several oedometer pressures for three cases of relative density (30%, 65% and 80%). The intersection between the dotted line and the curves allows us to find the transition content of the fines (F_{ct}). Tables 7, 8 and 9 present the values of the transition fines proportion for the three density cases. The transition fines content was determined using the equation of (Gudehus 1996) (Eq. 16), which showed that the maximum void ratio is not constant and depends on the effective stress.

$$e_i = e_{i0}\exp\left[-\left(\frac{3ps}{hs}\right)^n\right] \tag{16}$$

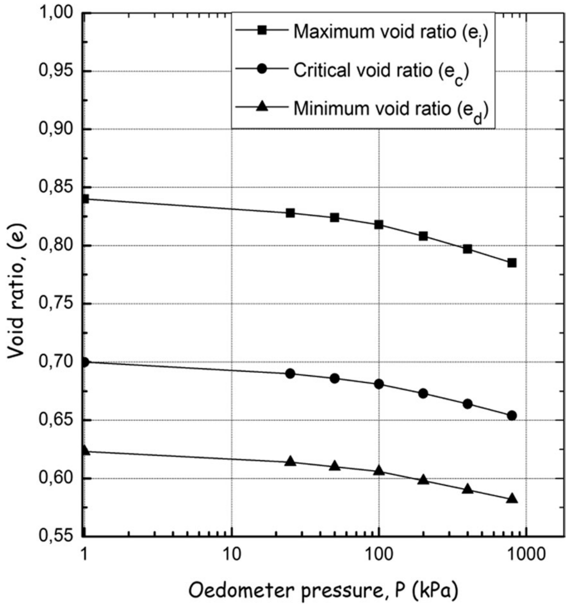

Fig. 15 variation of void ratio as a function of the oedometric pressure

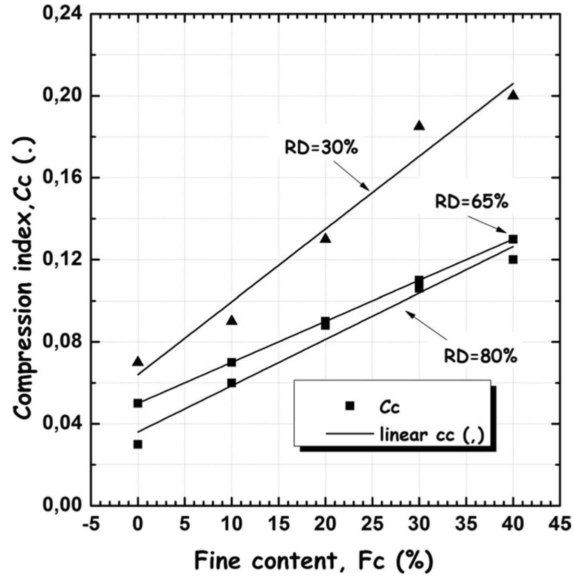

Fig. 16 variation of compression parameters as a function of the fines content

e_i maximum void ratio depends on the stress level, e_{i0} is the maximum void index at 0 stress level, hs is the granular hardness, n is the exponent and ps is the mean pressure.

Figure 15a shows the changes in the maximum void index, critical void index and minimum void index with the oedometer stress for the studied sand.

Gudehus (1996) suggests that there is a relationship between the initial maximum void index and the initial critical void index according to Eq. (17). Equation (18) shows the relationship between the initial critical void ratio and the critical void ratio which depends on the effective stress.

$$e_{i0} = 1.2e_{c0} \tag{17}$$

$$e_c = e_{c0} \exp\left[-\left(\frac{3ps}{hs}\right)^n\right] \tag{18}$$

Gudehus (1996) found a relationship between the maximal void index, the minimum void index and the critical void index Eq. (19).

$$\frac{e_i}{e_{i0}} = \frac{e_c}{e_{c0}} = \frac{e_d}{e_{d0}} = \exp\left[-\left(\frac{-tr\sigma}{hs}\right)^n\right] \tag{19}$$

We note from Tables 7, 8 and 9 that the transition fine content varied between 9.38 and 13.12% for the loose samples prepared at RD = 30%, 11.20% and 21.68% for the medium dense samples prepared at RD = 65%, and between 14.30% and 25.43% for the dense samples RD = 80%. For the three cases of relative density, the transitional fine content increases with the increase in the effective stress from 25 to 800 kPa. The increase in the transitional fine content with the increase in oedometer stress is due to the decrease in voids between the sand grains as the effective stress increases. The granular matrix (sand in this study) orients itself in a dense state which is favorable for the soil. The difference in the values of transitional fine content between the three relative densities is due to the difference between the initial void ratio, the specimen prepared at a relative density RD = 30% have a greater void ratio than those prepared at a relative density RD = 65% and RD = 80%, and this initial state has an effect on the values of the transitional fine content. It is clear from Tables 7, 8 and 9 that the transitional fines content decreases with the decrease in the maximum void ratio, which is unfavorable for

Table 10 Values of Compression parameters for sample with RD = 65% and RD = 80% as function as fines content

Percentage of fine content (%)	Compressibility index Cc for RD = 30%	Compressibility index Cc for RD = 65%	Compressibility index Cc for RD = 80%
0	0.070	0.052	0.031
10	0.091	0.072	0.060
20	0.130	0.090	0.080
30	0.185	0.110	0.106
40	0.200	0.133	0.120

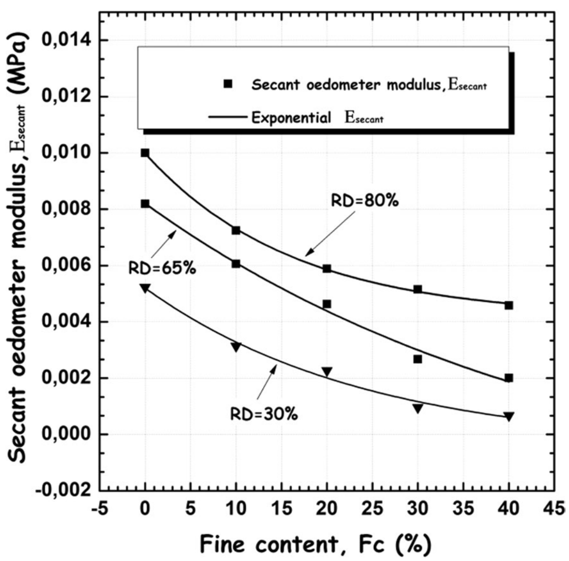

Fig. 17 Variation of secant oedometer modulus as a function of the fines content

the soil. For example, if we consider an oedometer stress of 25 kPa and a maximum void index of 0.84 (Tables 8) the fine content has a value of 15.69 (the sand will be dominant up to this value, after which the silt will dominate the behavior). on the other hand if we take the maximum void index of 0.785 the granular matrix will be dominant with a fine content of 11.20, and after this value the matrix of silt will dominate the behavior). Therefore, the decrease in the maximum void atio is unfavorable for the sand.

4.5 Impact of Fine Proportion on the Compression Parameters of Granular Chlef Soil

Figure 16 show the variation of the compressibility parameter Cc versus the fine content Fc, this parameter was determined from the compressibility curves and using the following equation:

$$C_c = \frac{\Delta e}{\Delta \log \sigma'} \tag{20}$$

The compressibility coefficient increases linearly with the addition of fine content for both cases of relative density, the compressibility coefficients for a relative density of 30% are greater than those for 65% and 80%, this difference in the compressibility coefficient is due to the difference in void ratio between the three relative densities, which are greater in the loose case (RD = 30%). The compressibility index Cc of the loose specimen (RD = 30%)

Table 11 Values of secant oedometer modulus for sample with RD = 30%, RD = 65% and RD = 80% as function as fines content

Percentage of fine content (%)	Secant oedometer modulus, E_{secant} (Mpa) for RD = 30%	Secant oedometer modulus, E_{secant} (Mpa) for RD = 65%	Secant oedometer modulus, E_{secant} (Mpa) for RD = 80%
0	52.30	81.90	100
10	31.40	60.61	72.46
20	22.70	46.30	55.82
30	09.56	26.73	51.54
40	06.74	20.17	45.87

is in the range of $0.070 < Cc < 0.200$, while for the medium dense specimen (RD = 65%) is in the range of $0.052 < Cc < 0.133$, and for the dense specimen (RD = 80%), the compressibility index Cc is in range of $0.031 < Cc < 0.120$. Based on the results, it can be concluded that the soil exhibits slight compressibility with a range of $0.03 < Cc < 0.20$. It can be observed from the results that the compressibility coefficients increase as the silt content increases from 0 to 40%. This difference attributed to the increase in the plasticity of the mixture, which increases with the increase in the quantity of fines. These studies reveal that the presence of silt has a negative effect on the liquefied Chlef soil. Table 10 shows the compressibility coefficient values for the different mixtures.

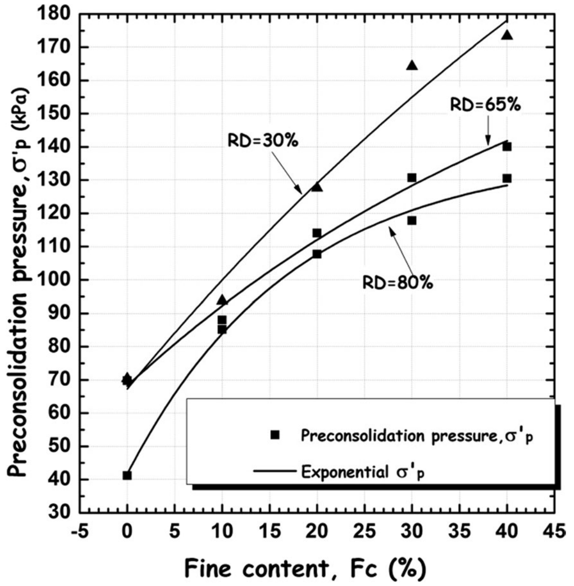

Fig. 18 variation of preconsolidation pressure as a function of the fines content

Figure 17 illustrates the variation of the secant oedometric modulus (E_{secant}). The secant oedometric E_{secant} module is another classic representation of soil compressibility in the oedometric test. It is defined by (Eq. 21):

$$E_{\sec ant\,(\sigma' va - \sigma' vb)} = \frac{\sigma' va - \sigma' vb}{Ha - Hb} H_i \tag{21}$$

H_a: height of sample at the end of the consolidation under oedometer stress σ'va.

H_b: height of sample at the end of the consolidation under oedometer stress σ'vb.

An Exponential decrease is observed in the secant oedometric modulus (E_{secant}) with the increase in fines content of sand.

It can be observed from Table 11 that an increase in density from 30 to 65% and from 65 to 80% leads to an improvement in the secant oedometric modulus from 52.30 to 81.90 MPa and from 81.90 to 100 MPa respectively, for clean sand. The increase in fine content induces a decrease in the secant oedometric modulus due to the increase in soil plasticity (increase in the quantity of silt in the sand). The following expressions are suggested to evaluate the secant oedometric modulus (E_{secant}), which is a function of the fines content (Fc):

$$E_{secant} = a \cdot Exp(-b \cdot Fc) + c \tag{22}$$

Figure 18 shows the variation of the preconsolidation pressure (σ'_p) versus fines content. An Exponential increase is observed in the preconsolidation pressure (σ'_p) with an increase in the silt content in sand. It is observed from Table 12 that as the compaction increases from 30 to 65% and from 65 to 80% the preconsolidation pressure (σ'_p) decreases from 70.36 to 69.75 kPa and from 69.75 to 41.17

Table 12 Values of preconsolidation pressure for sample with RD = 30%, RD = 65% and RD = 80% as function as fines content

Percentage of fine content (%)	Preconsolidation pressure (σ′p) (kPa) for RD = 30%	preconsolidation pressure (σ′p) (kPa) for RD = 65%	preconsolidation pressure (σ′p) (kPa) for RD = 80%
0	70.36	69.75	41.17
10	93.73	88.03	85.18
20	127.65	114.08	107.75
30	164.27	130.72	117.82
40	173.34	140.04	130.53

for clean sand respectively. The following expressions are suggested to evaluate the preconsolidation pressure (σ'_p), which is a function of the fines content (Fc):

$$\sigma_p' = a \cdot \mathrm{Exp}\,(-b \cdot Fc) + c. \tag{23}$$

5 Conclusion

Compressibility behavior of sand-silt mixtures was examined, in the first part, the effect of the fines content and relative density on the hypoplastic parameters model and the transition fines content were evaluated. then, the influence of relative density and silts proportion on the compression parameters of the liquefied Chlef sand was evaluated. The main conclusions that can be drawn are:

1. The relative density has a significant influence on the compressibility of the soil. Samples prepared at a loose state RD = 30% have larger void ratios and intergranular void ratios than the samples prepared at the dense state RD = 65% and 80%. Consequently, the coefficients of compressibility (C_c) and ($C_{c\text{-}s}$) are higher for the loose samples.
2. The fines content influences the calculation of the hypoplastic parameters of granular soils. An increase in the exponent α was observed with addition of silt proportion in chlef sand due to the decrease in $D_{50.}$ A reduction in the exponent β and the critical angle of friction φ_c was observed with the addition fine of content in chlef sand. The exponent n increases with increasing fine content and relative density from RD = 65 to RD = 80%.The granular hardness hs decrease with increasing fine content and relative density.The parameters e_i, e_d and e_c decreases with increasing oedometer pressure. These results can be used by researchers in the future to predict the behavior of sands containing fines during numerical simulations.
3. The results obtained showed that the hypoplastic model leads to results similar to those obtained experimentally in terms of void ratio in oedometer test and deviator-defroamtion response in triaxial test. α and β seem to have no effect on the compressibility curves and it was necessary to rely on their physical parameters. It was found that an increase in the α parameter increases the dilatancy of the curves in triaxial test.
4. The values of transition fines content (F_{ct})FC_t FC_t depend on the stress level and maximum void ratio calculated from hypoplastic parameters model. The decrease in the maximum void ratios results in a decrease in the value of the transition fine content, which is unfavorable for the soil, Therefore, this represents the worst case. Increasing the relative density from 30 to 80% increases the value of transition fine content and therefore the compression behavior of chlef sand-silt mixtures are improved. Soil samples in a loose state have smaller transition fine content values compared to those in medium and dense states, making them more susceptible to liquefaction
5. This study demonstrates that the compressibility parameters are influenced by the fine content and relative density. The increase of the fines content increases the compressibility parameter (C_c), C_{c-s} C_{c-s} this increase of the compressibility coefficients is due to the increase of fine fraction, which is itself more compressible than the sand-grained fraction. On the other hand, increasing the relative density from 30 to 80% reduces the compressibility coefficient (C_c) which is favorable for the soil.
6. The secant oeodmeter modulus E_{secant} decreases with an increase in fine content and increases with an increase relative density, while the preconsolidation pressure (σ'_p) increases with an increase in fine content and decreases as relative density decreases from 80 to 30%.

Based on our results, it can be concluded that increasing the fine content and relative density of sand significantly affects its liquefaction behavior (undrained behavior), hypoplastic parameters model (n, hs, α, φ_c and exponent β) and compression behavior (C_c C_c C_c, σ'_p and E_{secant}). These findings can be utilized for simulating coarse-grained soils mixed with fines.

Acknowledgements Ecole Nationale Supérieure d'Hydraulique de Blida, Chlef, Charles and Harbin university authors thank the reviewers for their detailed remarks. Tests were performed in the University Center of Ain Témouchent, Smart Structures Laboratory, Algeria and Institute of Hydrogeology, Engineering Geology and Applied Geophysics at UHBC University of Chlef and Charles University

Author Contributions DEB: Conceptualization, Methodology, Writing- original draft, Investigation. AB: Methodology, Conceptualization. FZB: Writing—review and editing. AK: Supervision, Methodology. AA: Conceptualization, Supervision, Methodology. JN: Data curation, Conceptualization. David Mašín: Data curation, Conceptualization.

Funding None.

Availability of Data Materials Not Applicable.

Declarations

Conflict of interest We declare that we have no financial and personal relationships with other person or companies that can inappropriately affect our work. There is no professional or other personal interest of any nature or kind in any product, service and/or company that could be construed as influencing the paper

References

Akhila M, Rangaswamy K, Sankar N (2019) Undrained response and liquefaction resistance of sand-silt mixtures. Geotech Geol Eng 37:2729–2745. https://doi.org/10.1007/s10706-018-00790-0

Amini F, Qi GZ (2000) Liquefaction testing of stratified silty sands. J Geotech Geoenviron Eng. https://doi.org/10.1061/(ASCE)1090-0241(2000)126:3(208)

Arab A, Shahrour I, Lancelot L (2011) A laboratory study of liquefaction of partially saturated sand. J Iber Geol 37(1):29–36

Arab A (2009) Monotonic and cyclic behaviour of silty sand. C R Mec 337:621–631

Arab A, Sadek M, Belkhatir M, Shahrour I (2014) Monotonic preloading effect on the liquefaction resistance of Chlef Silty sand. Arab J Sci Eng 39:685–694

ASTM D 2435/ D 2435M. (1997) Standard test method for one dimensional consolidation properties of soil using incremental loading, Annual Book of ASTM Standards, American Society for Testing and Materials, West Conshohocken, PA 19428

ASTM D 4253-00 (2002) Standard test method for maximum index density and unit weight of soils using a vibratory table. Annual Book of ASTM Standards, American Society for Testing and Materials, West Conshohocken, pp 1–14

ASTM D 4254-00 (2002) Standard test method for minimum index density and unit weight of soils and calculation of relative density. Annual Book of ASTM Standards, American Society for Testing and Materials, West Conshohocken, pp 1–9

Belhassena FZ, Liang T, Eddine BD, Chunhui L, Xianzhang L (2021) Estimation of bending moment and pile displacement for soil-pile-quay wall system subjected to liquefaction induced lateral spreading. Soil Dyn Earthq Eng 151:106989. https://doi.org/10.1016/j.soildyn.2021.106989

Belkhatir M, Arab A, Della N, Missoum H, Schanz T (2010) Influence of intergranular void ratio on monotonic and cyclic undrained shear response of sandy soils. CR Mec 338:290–303

Belkhatir M, Arab A, Schanz T, Missoum H, Della N (2011) Laboratory study on the liquefaction resistance of sand-silt mixtures: effect of grading characteristics. Granul Matter 13:599–609

Belkhatir M, Arab A, Della N, Schanz T (2012) Experimental study of undrained shear strength of silty sand: effect of fines and gradation. Geotech Geol Eng 30(5):1103–1118

Benahmed N, Canou J, Dupla JC (1999) Influence of the initial conditions and the type of loading on the stability of the undrained behavior of loose sand. In: CR 12th Europian conference of soil mechanics and foundations engineering, Amsterdam (2), pp 687–690

Bouri D, Krim A, Brahim A, Arab A (2019) Shear strength of compacted Chlef sand: effect of water content, fines content and others parameters''. Stud Geotech Mech. https://doi.org/10.2478/sgem-2019-0027

Bouri DE, Brahimi A, Krim A, Arab A, Najser J, Mašín D (2021) Compression behaviour of Chlef sand and transition of fines content using pressure-dependent maximum void ratios of sand. Geotech Geol Eng. https://doi.org/10.1007/s10706-021-01985-8

Brahim A, Arab A, Belkhatir M, Shahrour I (2016) Laboratory study of geotextiles performance on reinforced sandy soil. J Earth Sci 27(6):1060–1070

Brahim A, Arab A, Marwan S, Shahrour I (2018) Laboratory investigation of the influence of geotextile on the stress-strain and volumetric change behavior of sand. Geotech Geol Eng. https://doi.org/10.1007/s10706-018-0446-6

Brahimi A, Bouri DE, Boutaraa Z, Nougar B, Krim A, Chemmam M, Arab A (2023) Numerical and experimental study on the efect of fber reinforcement on the shear strength and hydraulic conductivity of Chlef soil. Innov Infrastruct Solut. https://doi.org/10.1007/s41062-022-01011-7

Cabalar AF, Hasan RA (2013) Compressional behaviour of various size/shape sand–clay mixtures with different pore fluids. Eng Geol 164:36–49

Castro.G (1969) Liquefaction of sands. PhD thesis, Harvard University, Cambridge, USA

Chang M, Kuo CP, Hsu R, Shau S, Lin T (2012) Liquefaction potential and post-liquefaction settlement evaluations of the Chuoshui River Alluvial Fan in Taiwan. Bull Eng Geol Environ 71:325–336

Chen QS, Wang CF, Juang CH (2016) Probabilistic and spatial assessment of liquefaction-induced settlements through multiscale random field models. Eng Geol 211:135–149. https://doi.org/10.1016/j.enggeo.2016.07.002

Cfa A, Bernard O, Seth ON, Kwabena OO (2013) The influence of observed clay content on shear strength and compressibility of residual sandy soils international. J Eng Res Appl (IJERA) 3(4):2538–2542

Covert KM, Yamamuro JA (1997) Static liquefaction of silty sands. In: 5th great lakes geotechnical/geoenvironmental Conference, Michigan, pp 1–20

Della N, Belkhatir M, Arab A, Canou J, Dupla JC (2015) Undrained monotonic response and instability of medium-dense sandy soil. Mar Georesour Geotechnol

33(6):487–495. https://doi.org/10.1080/1064119X.2014.954175
Djafar Henni A, Arab A, Belkhatir M, Hamoudi SA, Khelafi H (2013) Undrained behavior of silty sand: effect of the overconsolidation ratio. Arab J Geosci 6(2):297–307
Enomoto T (2019) Liquefaction and post-liquefaction properties of sand-silt mixtures and undisturbed silty sands. Soil Found 59:2311–2323
Ghani S, Kumari S (2021) Insight into the effect of fine content on liquefaction behavior of soil. Geotech Geol Eng. https://doi.org/10.1007/s10706-020-01491-3
Goudarzy M, Sarkar D, Lieske W, Wichtmann T (2022) Influence of plastic fines content on the liquefaction susceptibility of sands: monotonic loading. Acta Geotech 17:1719–1737. https://doi.org/10.1007/s11440-021-01283-w
Gudehus G (1996) A comprehensive constituve equation for granular materials. Soils Found 36(1):1–12
Herle I, Gudehus G (1999) Determination of parameters of a hypoplastic constitutive model from properties of grain assemblies. Mech Cohes Frict Checkout 4:461–486
Huang YT, Huang AB, Kuo YC (2004) Tsai MD (2004) A laboratory study on the undrained strength of a silty sand from central Western Taiwan. Soil Dyn Earthq Eng 24:733–743
Ishihara K, Yasuda S, Yoshida Y (1990) Liquefaction-induced flow failure of embankments and residual strength of silty sands. Soils Found 30(3):69–80
Ishihara K (1993) Liquefaction and flow failure during earthquakes. Geotechnique 43(3):351–415
Kuerbis R, Negussey D, Vaid YP (1988) Effect of gradation and fine content on the undrained response of sand. Hydraulic Fill Structure, vol 21, pp 330–345. Geotechnical Special Publication, ASCE, New York
Krim A, Brahimi A, Arab A, Bouri DE, Marwan S (2021) A laboratory study of shear strength of partially saturated sandy soil. Geomech Geoeng. https://doi.org/10.1080/17486025.2020.1864034
Lade PV, Yamamuro JA (1997) Effects of non-plastic fines on static liquefaction of sands. Can Geotech J 34:918–928
Lupogo K (2012) Effect of fines mineralogy on the oedometric compressional behavior of sandy soils. J Civ Eng Construct Technol 4(7):232–238
Madabhushi GSP, Haigh SK (2010) Liquefaction induced settlement of structures. In: International conferences on recent advances in geotechnical earthquake engineering and soil dynamics, p 5
Mahmoud Y, Cherif Taiba A, Hazout L, Belkhatir M (2022) Comprehensive laboratory study on stress-strain of granular soils at constant global void ratio: combined effects of fabrics and silt content. Acta Geotech. https://doi.org/10.1007/s11440-02201480-1
Mase LZ (2020) Seismic hazard vulnerability of Bengkulu City, Indonesia, based on deterministic seismic hazard analysis. Geotech Geol Eng 38(5):5433–5455. https://doi.org/10.1007/s10706-020-01375-6
Mase LZ, Agustina S, Farid M, Supriani F, Tanapalungkorn W, Likitlersuang S (2023) Application of simplified energy concept for liquefaction prediction in Bengkulu City, Indonesia. Geotech Geol Eng. https://doi.org/10.1007/s10706-023-02388-7
Mašín D (2012a) Asymptotic behaviour of granular materials. Granul Matter 14(6):759–774
Masin D (2019) Modeling of soil behaviour with hypoplasticity. Springer series in geomechanics and geoengineering
Mohammadi-Haji B, Ardakani A (2020) Calibration of a hypoplastic constitutive model with elastic strain range for Firoozkuh sand. Geotech Geol Eng. https://doi.org/10.1007/s10706-020-01363-
Monkul MM, Onal O (2006) A visual basic program for analyzing oedometer test results and evaluating intergranular void ratio. Comput Geosci Elsevier Sci 32:696–703
Monkul M, Ozden G (2007) Compressional behaviour of clayey sand and transition fines content. Eng Geol 89:195–205
Monkul MM, Ehsan E, Aykut Ş (2017) Coupled influence of content, gradation and shape characteristics of silts on static liquefaction of loose silty sands. Soil Dyn Earthq Eng 101:12–26
Najjar SS, Yaghi K, Adwan M, Jaoude AA (2015) (2015) Drained shear strength of compacted sand with clayey fines. Int J Geotech Eng 9(5):513–520
Najser J, Mašín D, Bohác J (2012) Numerical modelling of lumpy clay landfill. Int J Numer Anal Meth Geomech 36:17–35. https://doi.org/10.1002/nag.990
Nougar B, Brahimi A, Bouri DE, Arab A, Benessalah I (2021) Laboratory Investigation into the Effect of Fines Plasticity on the Mechanical Behavior of Sand/Fines Mixtures. Transp Infrastruct Geotechnol. https://doi.org/10.1007/s40515-020-00144-5
Nougar B, Bouri DE, Brahimi A, Belhassena FZ, Arab A (2022) Effect of plastic fine and non-plastic fine on the compressibility behavior of granular material. Arab J Geosci. https://doi.org/10.1007/s12517-022-10980-z
Porcino DD, Diano V, Triantafyllidis T, Wichtmann T (2019) Predicting undrained static response of sand with non-plastic fines in terms of equivalent granular state parameter. Acta Geotech. https://doi.org/10.1007/s11440-019-00770-5
Rahman M, Lo S (2014) Undrained behavior of sand-fines mixtures and their state parameter. J Geotech Geoenviron Eng 140(7):04014036. https://doi.org/10.1061/(ASCE)GT.1943-5606.0001115
Thevanayagam S (1998) Effect of fines and confining stress on undrained shear strength of silty sands. J Geotech Geoenviron Eng Div ASCE 124(6):479–491
Thevanayagam S, Mohan S (2000) Inter-granular state variables and stress-strain behaviour of silty sands. Geotechnique 50(1):1–23
Thevanayagam S, Martin GR (2002) Liquefaction in silty soils-screening and remediation issues. Soil Dyn Earthq Eng 22(9–12):1035–1042
von Wolffersdorff PA (1996) A hypoplastic relation for granular materials with a predefined limit state surface. Mech Cohesive-Frict Mater. https://doi.org/10.1002/(SICI)10991484(199607)1:3%3c251::AID-CFM13%3e3.0.CO;2-3
Yin JH (1999) Properties and behaviour of Hong Kong marine deposits with different clay contents. Can Geotech J 36(6):1085–1095
Zlatovic S, Ishihara K (1995) On the influence of non-plastic fines on residual strength. In: Proceedings of the first

international conference on earthquake geotechnical engineering. Tokyo, pp 14–16